Analyst

Accepted Manuscript

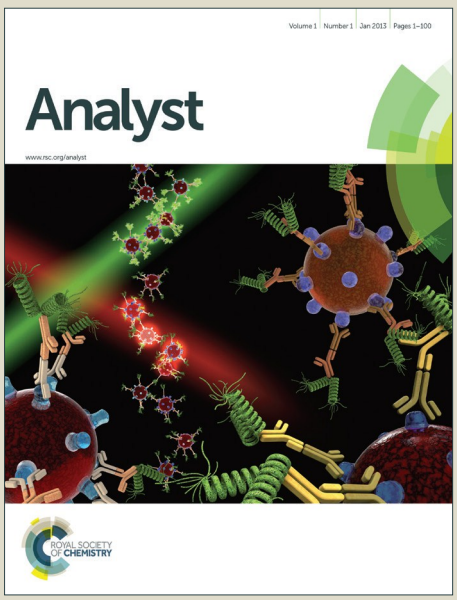

ROYAL SOCIETY OF CHEMISTRY

www.rsc.org/analyst

Analyst

COMMUNICATION

Gold Nanosponges (AuNS): A Versatile Nanostructure for Surface Enhanced Raman Spectroscopic Detection of Small Molecules and Biomolecules

Received 00th January 20xx,
Accepted 00th January 20xx

DOI: 10.1039/x0xx00000x

www.rsc.org/

Gregory Q. Wallace, Mariachiara S. Zuin, Mohammadali Tabatabaei, Pierangelo Gobbo, François Lagugné-Labarthet, and Mark S. Workentin*

Prepared by simple pour and mix chemistry, gold nanosponges (AuNS) are versatile structures for surface-enhanced Raman spectroscopy (SERS). An investigation into the enhancement is performed by relating the nanostructure's morphology to the SERS signal. The potential of the AuNS in SERS-based molecular and biomolecular detection is introduced.

Overcoming the intrinsically weak Raman process via a combination of electromagnetic[1] and chemical enhancement mechanisms,[2] surface-enhanced Raman spectroscopy (SERS) provides enhancements of several orders of magnitude.[3] The generation of nanoscale regions of electromagnetic enhancement, known as "hot-spots", dominates the SERS enhancement.[4] A wide range of structures have been developed for SERS, with emphasis on both top-down and bottom-up fabrication methods to tailor the hot-spots for a given set of experimental conditions. Top-down approaches rely on lithographic techniques, such as electron beam (EBL),[5] nanoimprint,[6] and nanosphere lithographies (NSL).[7] Although these methods can produce reliable structures with a consistent distribution of hot-spots, and sub-femtomolar limits of detection,[8, 9] the necessary equipment, costs, and training associated with these techniques often makes them less desirable.[10] On the other hand, bottom-up fabrication techniques are often considerably more time- and cost-effective. By adjusting the synthetic approaches, researchers have produced nanostructures ranging from simple rough nanoparticles[11] to more complex structures including nanorattles,[12] trisoctahedrons,[13] and nanostars[14, 15] all with intrinsic hot-spots. It is important to note that additional hot-spots are formed when the nanostructures are in close proximity to each other.[16]

Currently, one of the greatest challenges in the synthesis of gold nanoparticles is the development of biocompatible synthetic pathways. The main challenge during the synthesis is to promote a controlled reduction of the gold salt precursor, usually $HAuCl_4 \cdot 3H_2O$, without employing harsh reducing agents, such as $NaBH_4$ and $LiAlH_4$.[17] A variety of synthetic methods have been developed to overcome this,[18-21] with recent developments including the combined reducing effect of hydrogen peroxide (H_2O_2) and (2-(N-morpholino) ethanesulfonic acid (MES).[22] This method is a simple, one-pot synthesis that uses "green" chemistry, and most importantly is biocompatible. In a typical synthesis, concentrations of H_2O_2 in the range 20-140 μM are added to a 100 μM solution of $HAuCl_4 \cdot 3H_2O$ in 1 mM MES (pH 6.5). By the naked eye, a fast colour change of the solution from colourless to blue can be observed for concentrations of H_2O_2 lower than 110 μM, and a subsequent progress in the colour change to purple and finally red for concentrations of H_2O_2 higher than 110 μM. Transmission electron microscopy (TEM) images of different samples at different H_2O_2 concentrations showed that the red colour is due to small nanoparticles (AuNP) with 5-15 nm diameters, while purple and blue solutions instead contain larger and rougher gold nanostructures that resemble nanosponges (AuNS). The colour change from blue to red using such a narrow range of H_2O_2 concentration, allowed De La Rica and coworkers to develop the plasmonic enzyme-linked immunosorbent assay (ELISA) for the naked eye detection of prostate specific antigen and HIV-1 capsid antigen p24.[22] However, it was noticed that for concentration lower than 100 μM in H_2O_2 the redox reaction between H_2O_2, MES and $HAuCl_4 \cdot 3H_2O$ is not complete and in the time scale of minutes the blue solutions were turning to red, indicating a slow disaggregation of AuNS into 5-15 nm AuNP.[23] The lack of control over the colour shift represented a major issue for the assay, causing potential false-negative results. Nevertheless, it could be solved by the addition of a thiol (namely glutathione – GSH) 10 minutes after the starting of the redox reaction that binds to the gold core and stabilizes the AuNS. This quenching step was subsequently adopted in the general protocol for the

[a] Department of Chemistry, and the Centre for Advanced Materials and Biomaterials Research, The University of Western Ontario, 1151 Richmond St. London ON, Canada, N6A 5B7. Email: mworkent@uwo.ca

Electronic Supplementary Information (ESI) available: Experimental Section and additional TEM and AFM images. See DOI: 10.1039/x0xx00000x

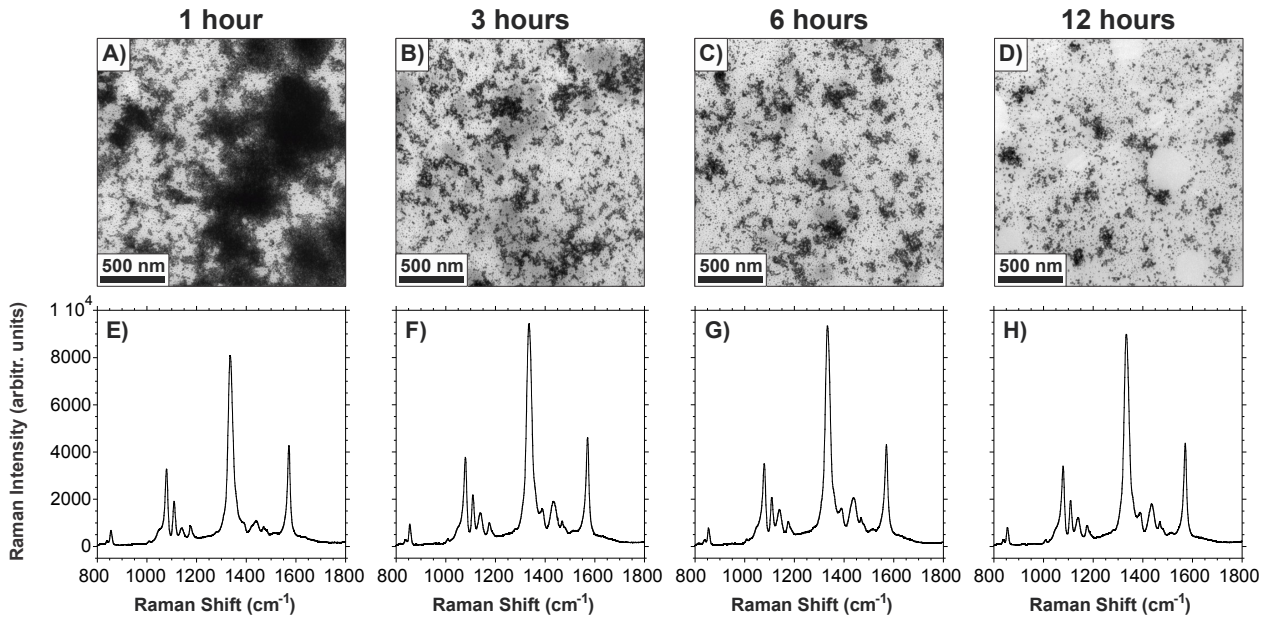

Fig. 1 Analysis of 4-NTP quenched AuNS by TEM (A-D) and by spot SERS analysis (E-H) for reaction times of 1, 3, 6, and 12 hours. All reactions were quenched with a 3 mM solution of 4-NTP and exposed to the 4-NTP for 1 hour. For the SERS spectra, a 5 sec. acquisition time was used with no baseline correction.

plasmonic ELISA sensor.[24] Beyond the development of plasmonic ELISA sensors, the synthetic protocol has been adapted for the detection of glucose,[25] thus introducing the structure for biosensing of small molecules. Here, the H_2O_2 necessary for the reduction of the $HAuCl_4 \cdot 3H_2O$ was generated via the oxidation of glucose by glucose oxidase. It was found that the intensity of the plasmon resonance light scattering increased with the concentration of glucose, therefore yielding an increase of the H_2O_2 concentration.

With a short and simple synthesis, coupled with interesting physical and chemical characteristics of the nanostructure, it was believed that the AuNS could potentially be used for applications in SERS including molecular and biomolecule detection. To determine if this was true and to what extent, a series of proof of concept studies were performed. First, the integration of a small molecule Raman reporter to the synthesis of the AuNS allowed for determining the extent of the Raman enhancement. Through a series of SERS measurements coupled with TEM and atomic force microscopy (AFM), the structure of the AuNS and the means by which enhancement occurs are determined. Subsequently, a comparison between the SERS of the AuNS and standard 20 nm AuNP[26] was performed to highlight the benefit of the AuNS with respect to one of the most used bottom-up SERS structures. Lastly, by further modifying the synthesis to include a strategically designed peptide that acts as a Raman reporter, the potential for SERS-based biomolecule detection using the AuNS is demonstrated.

To stop the reduction of $HAuCl_4$ during the synthesis of the AuNS, a quenching thiol was required. In a previous study of the AuNS, GSH was used,[23] however, for the purpose of this work, it was substituted for 4-nitrothiophenol (4-NTP). 4-NTP has been studied by SERS[27, 28] as it provides a strong non-resonant SERS signal making it an ideal molecule for testing the SERS compatibility of the AuNS. The details for the synthesis of the AuNS can be found in the ESI.

One of the key features of the AuNS synthetic procedure is that by varying the time prior to the addition of the quenching thiol (4-NTP), the structural characteristics, notably size and morphology, along with the related chemical properties can be tuned. It is therefore important to optimize the synthetic conditions in order to obtain the size of the AuNS size that yields the greater Raman enhancement. For this purpose, a series of AuNS were synthesized by quenching the redox reaction at different times: 1, 3, 6, and 12 hours. The corresponding TEM images in Figure 1A-D highlight that as the redox reaction proceeds, the sizes of the AuNS aggregates vary from micrometres (Figure 1A) to 50-100 nm (Figure 1D) indicating more isolated AuNS. These results are consistent with those obtained using GSH as the quenching thiol.[23] The AuNS were then washed with MilliQ water using centrifugal filtering devices (50 kDa MWCO) and the SERS samples were prepared by drop-casting 160 µL of the corresponding as-obtained AuNS solutions directly onto clean microscope cover slips. The cover slips were then rinsed with dry ethanol to remove any residual starting materials. The samples were then analyzed by SERS using a 0.9 N.A. ×100 objective. As such, according to the TEM images, large groupings of AuNS are probed for each spot analysis, as opposed to isolated AuNS. Based on the average results of 15 spot analyses per sample (Figure 1E-H), a higher SERS enhancement was observed for the 3 hours sample with respect to the 1 hour sample. Even though the gain of the Raman intensity was around 5%, further experiments were conducted using a synthesis time of 3 hours for optimal experimental conditions. As the reaction time is further increased, no additional enhancement is observed. Overall, a balance between total time of synthesis and the observed SERS signal was observed for AuNS with a reduction

time of 3 hours, although much shorter times can be used without significant decrease in signal intensity.

A reduction time of 3 hours for the synthesis of the AuNS is comparably longer than the 5 minute reduction times that have previously been reported for the syntheses of metallic NS.[29, 30] However, the synthesis described by Krishna *et al.* requires the use of $NaBH_4$ as a reducing agent.[29] As mentioned earlier, this limits the biocompatibility of the synthesis. The synthesis of the bimetallic NS of Liu *et al.* does not require the use of harsh reducing agents, however, it requires the use of heating at 100 °C for 12 hours, followed by cooling before washing and centrifugation.[30] Our synthesis is completed entirely at room temperature, and overall, takes less time. A reduction time comparable with ours has recently been reported.[31] Although these NS could be synthesized as mono or heterometallic, it is necessary to freeze dry the NS to maximize loading of the molecule of interest. As is the case for the other metallic NS, the probe molecule is added after the synthesis is completed, a step that is not required for the synthesis of our AuNS as the probe molecule is used to quench the reaction.

The samples was then analysed in greater detail through AFM and TEM. AFM shows complex rough structures that range from isolated ~60 nm in diameter to a few hundreds of nanometres (Fig. S1A, ESI) with isolated heights between 20 and 30 nm (Fig. 2A). On the other hand, TEM images show that these structures are themselves comprised of multiple 10-30 nm gold cores self-assembled into larger structures (Fig. S1B, ESI). It is the close proximity of the gold cores (<10 nm) which is responsible for the SERS enhancement. Since the probed areas contain multiple AuNS, each with multiple cores, a multiplicative effect for the enhancement occurs. This is not the case when preparing SERS platforms by NSL, as the hot-spots are localized to tips of adjacent nanotriangles[32] or nanopyramids,[27] or within the hole of a nanohole array.[33] As these types of structures are often larger (>100 nm), fewer of them are illuminated using the same beam diameter that what used in this study. It is noteworthy that following a typical synthetic protocol for the AuNS, a total volume of 3 mL is prepared, resulting in one vial providing 18 SERS samples. Considering that multiple vials can be easily prepared at a time, the total number of samples that could be made is far greater than the amount that could be fabricated using other techniques (i.e. EBL or NSL) in the same length of time.

To better understand how and where the hot-spots were generated, SERS maps were collected on nanosponges deposited over a glass coverslip. For the SERS mapping, a 1.4 N.A. ×100 objective providing a beam diameter at the sample of ~0.8 µm was used. Raman mapping of the samples were acquired using a micromotorized stage and collecting step spectra every 0.75 µm along the x and y directions with an integration time of 1s per spectrum. Figure 2A shows an AFM image of aggregates of AuNS overlaid with a (10x10) μm^2 integrated Raman map in the 1300-1350 cm^{-1} spectral range, corresponding to the symmetric stretching of the NO_2 group. Spectrum 1 in Figure 2B corresponds to region 1 in Figure 2A, highlighting that where the AuNS are not present, little to no Raman signal is observed, indicating that signal intensity is directly related to the surface enhancement effect exerted by the AuNS (spectrum 2). It also shows that the higher signal intensity is related to those areas that contain a larger density of AuNS within the probed areas. It is noteworthy that as the collection of AuNS are formed, an increase in height can be observed (Figure 2C, see Fig. S2 ESI). Such regions, where the height is greater than 100 nm (indicated by the circle in Figure 2C), hinder the enhancement, resulting in a lessened SERS signal (Figure 2D). These large aggregates were very common in the 1 hour sample, which correlates to the lower signal observed in Figure 1E.

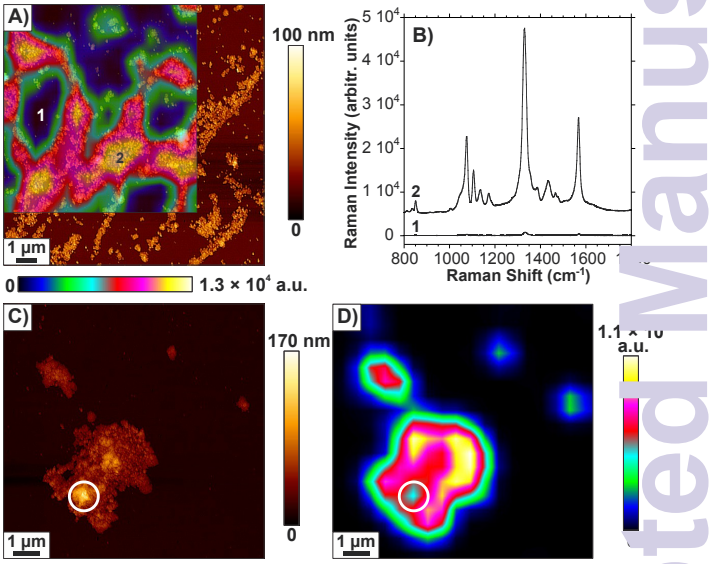

Fig. 2 Analysis of 4-NTP quenched AuNS by A) AFM phase imaging, B) TEM, C) AFM height and overlaid SERS mapping from 1300 – 1350 cm-1 where spots 1 and 2 correspond to the SERS spectra in D). For the SERS spectra, a 1 sec. acquisition time was used with no baseline correction.

Subsequently, we compared the AuNS with the commonly used 20 nm AuNP[26] to determine which structure provided better SERS activity. Citrate-capped AuNP with a diameter of 20 nm were functionalized with 4-NTP (see ESI). This step was regulated so as to have similar amounts of 4-NTP present for both the AuNS and the AuNPs by keeping the ratio between the thiol and the $HAuCl_4 \cdot 3H_2O$ constant.

The comparison between the SERS of 4-NTP on AuNS and AuNP is reported in Figure 3. In the figure, the maxima, minima, and average from an analysis of 20 points are reported for each nanostructure and show evidently greater signal intensity (30-40%) for the AuNS with respect to the AuNP. More importantly, the synthesis of the AuNP requires proper equipment and glassware, whereas the entire synthesis of the AuNS can be performed in a single vial through simple pour and mix chemistry, and takes only a few hours to complete. Furthermore, unlike the AuNS, the addition of the thiol of interest occurs after the citrate-capped AuNP have been prepared. As performed, the synthesis of the 4-NTP-capped 20 nm AuNP is more than 3 times longer than the synthesis of the AuNS. Together with a stonger SERS response

these results confirm the advantages of the AuNS compared to the traditional 20 nm AuNP.

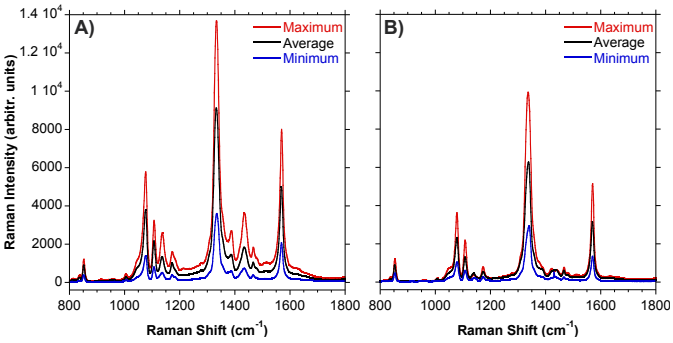

Fig. 3 SERS comparison between A) 4-NTP quenched AuNS, and B) AuNPs prepared by the Turkevich method capped with 4-NTP. For the SERS spectra, a 5 sec. acquisition time was used with no baseline correction.

In the aforementioned studies involving metallic NS, none explored the potential role of NS in biosensing,[29-31] instead focussing solely on the SERS potential using either Rhodamine 6G or Rhodamine B as the probe molecule. To illustrate the biocompatibility of the synthesis, along with the possibility of our AuNS being used for SERS-based biomolecule detection applications, a short peptide (KFFKFFC) was synthesized. The peptide was used in place of 4-NTP for quenching the redox process after 3 hours. This step was to be achieved by the thiol of cysteine (shown in red in the structure of the peptide as the inset in Fig. 4A) attaching to the AuNS, forming a gold-thiolate linkage. The peptide functionalized AuNS were washed with Milli-Q water using centrifugal filtering devices (50 kDa MWCO) and 160 µL of AuNS solution were drop-casted onto the cover slip and rinsed with dry ethanol to remove any residual starting material. The Raman spectrum of cysteine has previously been studied, and contains two peaks at 2542 and 2552 cm^{-1}, corresponding to the S-H stretch.[34] The SERS spectrum of the peptide quenched AuNS (Figure 4A) does not contain any peaks from 2400-2700 cm^{-1} (highlighted in red in the spectrum), indicating that the peptide formed a thiolate linkage with the surface of the AuNS. The second important feature of the KFFKFFC peptide, was the presence of four phenylalanine residues (shown as green in the structure of the peptide). Phenylalanine has a distinct peak to all other amino acids at 1005 cm^{-1}, corresponding to the deformation of the aromatic ring.[35] Aromatic rings are often a key feature of model Raman and SERS molecules, such as 4-NTP, due to their large Raman scattering cross-section.[36] Biomolecules tend to have small Raman scattering cross-sections, thus making them difficult to detect by SERS. Incorporating 4 phenylalanine residues overcomes this traditional limitation, due to the aromatic ring of each residue. Therefore, this peptide is an good Raman reporter for SERS studies involving biosensing. In Figure 4A, a distinct peak is observed at 996 cm^{-1} (highlighted green in the spectrum), which coincides with the deformation of the phenylalanine aromatic ring. Since the peak has a strong intensity, SERS maps were generated by integrating the vibrational mode from 980-1005 cm^{-1} (Figure 4B). As in the case with 4-NTP, the regions without any AuNS (highlighted 1 in Figure 4B) show no starting material (spectrum 1 in Figure 4C). Furthermore, the areas with the greatest amount of AuNS within the probed region show the greatest intensity for the phenylalanine peak (spectrum 2 in Figure 4C). Such similarities between the 4-NTP, and peptide quenched AuNS highlights the possibility of the AuNS being used for SERS-based biosensing applications.

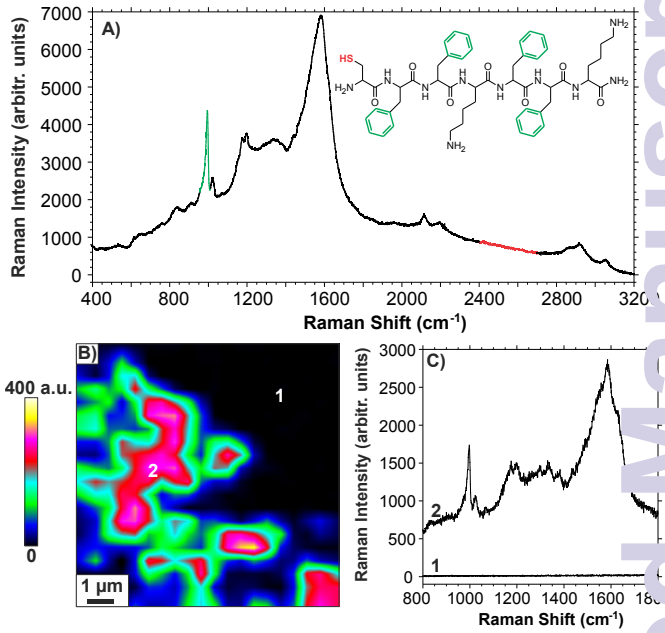

Fig. 4 SERS analysis of peptide quenched AuNS. A) Single point analysis, with acquisition time of 10 sec. with the structure of the peptide included as an inset. B) SERS maps generated by integrating from 980 – 1005 cm-1 where spots 1 and 2 correspond to the spectra in C) with a 1 sec. acquisition time. For the SERS spectra, no baseline correction was applied.

In this presented work, we introduced a means of adapting the synthesis of AuNS for SERS. Existing syntheses of metallic NS rely on the formation of an uncontrolled aggregate of reduced precursor without the probe molecule on the surface.[29-31] As was shown in this work, the formation of large aggregates, those with heights greater than 100 nm, have a lessened SERS intensity relative to those that are less aggregated. Overall, thanks to the quick preparation, ease of synthesis, ability to control the size of the nanostructure, and high SERS signal, the AuNS shown represent an extremely efficient and versatile nanostructure for SERS. The potential use of the AuNS for SERS-based biomolecule detection was introduced by integrating a Raman reporter peptide to the synthesis as a means of quenching the reaction. Once the peptide was attached to the surface of the AuNS, direct detection was possible. The use of AuNS for direct or indirect detection of biomolecules should further be evaluated in particular when the probe molecules are unable to quench the reduction is currently being investigated. The versatile synthesis can potentially be further adapted to include both a cellular recognition peptide and a Raman reporter on the surface of the AuNS. This way, the AuNS could be used for both in vitro and in vivo studies involving SERS. This is

application that may not be possible with the other metallic NS as the size of the aggregates are quite large.

We thank the lab of Dr. Robert H.E. Hudson for their assistance with the peptide. This research was supported by NSERC (Canada) and the University of Western Ontario. This research was also funded by the Canada Research Chairs program in "Photonics and Nanosciences" (FL-L). PG thanks the Vanier CGS and Research Western for funding.

Notes and references

1 D. L. Jeanmaire and R. P. Van Duyne, *J. Electroanal. Chem.*, 1977, **84**, 1-20.
2 M. G. Albrecht and J. A. Creighton, *J. Am. Chem. Soc.*, 1977, **99**, 5215-5217.
3 E. C. Le Ru and P. G. Etchegoin, *MRS Bulletin*, 2013, **38**, 631 640.
4 S. M. Morton, D. W. Silverstein and L. Jensen, *Chem. Rev.*, 2011, **111**, 3962-3994.
5 A. Gopalakrishnan, M. Chirumamilla, F. De Angelis, A. Toma, R. P. Zaccaria and R. Krahne, *ACS Nano*, 2014, **8**, 7986-7994.
6 C. Leordean, A.-M. Gabudean, V. Canpean and S. Astilean, *Analyst*, 2013, **138**, 4975-4981.
7 D. Volpati, E. R. Spada, C. C. P. Cid, M. L. Sartorelli, R. F. Aroca and C. J. L. Constantino, *Analyst*, 2015, **140**, 476-482.
8 G. Q. Wallace, M. Tabatabaei and F. Lagugné-Labarthet, *Can. J. Chem.*, 2014, **92**, 1-8.
9 M. Tabatabaei, M. Najiminaini, K. Davieau, B. Kaminska, M. R. Singh, J. J. L. Carson and F. Lagugné-Labarthet, *ACS Photonics*, 2015, **2**, 752-759.
10 N. Marquestaut, A. Martin, D. Talaga, L. Servant, S. Ravaine, S. Reculusa, D. M. Bassani, E. Gillies and F. Lagugné-Labarthet, *Langmuir*, 2008, **24**, 11313-11321.
11 S. Wu, X. Zhou, X. Yang, Z. Hou, Y. Shi, L. Zhong, Q. Jiang and Q. Zhang, *J. Nanopart. Res.*, 2014, **16**, 1-13.
12 A. Jaiswal, L. Tian, S. Tadepalli, K.-k. Liu, M. Fei, M. E. Farrell, P. M. Pellegrino and S. Singamaneni, *Small*, 2014, **10**, 4287-4292.
13 Q. Zhang, N. Large and H. Wang, *ACS Appl. Mater. Interfaces*, 2014, **6**, 17255-17267.
14 C. G. Khoury and T. Vo-Dinh, *J. Phys. Chem. C*, 2008, **112**, 18849-18859.
15 P. Ndokoye, J. Ke, J. Liu, Q. Zhao and X. Li, *Langmuir*, 2014, **30**, 13491-13497.
16 S. L. Kleinman, B. Sharma, M. G. Blaber, A.-I. Henry, N. Valley, R. G. Freeman, M. J. Natan, G. C. Schatz and R. P. Van Duyne, *J. Am. Chem. Soc.*, 2013, **135**, 301-308.
17 A. C. Templeton, W. P. Wuelfing and R. W. Murray, *Acc. Chem. Res.*, 2000, **33**, 27-36.
18 M. Anderson, E. Torres-Chavolla, B. Castro and E. Alocilja, *J. Nanopart. Res.*, 2011, **13**, 2843-2851.
19 K. Sathish Kumar, R. Amutha, P. Arumugam and S. Berchmans, *ACS Appl. Mater. Interfaces*, 2011, **3**, 1418-1425.
20 M. Gkikas, J. Timonen, J. Ruokolainen, P. Alexandridis and H. Iatrou, *J. Polym. Sci., Part A: Polym. Chem.*, 2013, **51**, 1448-1456.
21 S. Pandey, G. K. Goswami and K. K. Nanda, *Carbohydr. Polym.*, 2013, **94**, 229-234.
22 R. de la Rica and M. M. Stevens, *Nat. Nanotech.*, 2012, **7**, 821-824.
23 P. Gobbo, M. J. Biondi, J. J. Feld and M. S. Workentin, *J. Mater. Chem. B*, 2013, **1**, 4048-4051.
24 D. Cecchin, R. de la Rica, R. E. S. Bain, M. W. Finnis, M. M. Stevens and G. Battaglia, *Nanoscale*, 2014, **6**, 9559-9562.
25 W. B. Wu, L. Zhan, J. Wang and C. Z. Huang, *Anal. Methods*, 2014, **6**, 3779-3783.
26 J. Turkevich, P. C. Stevenson and J. Hillier, *Discuss. Faraday Soc.*, 1951, **11**, 55-75.
27 M. Tabatabaei, A. Sangar, N. Kazemi-Zanjani, P. Torchio, A. Merlen and F. Lagugné-Labarthet, *J. Phys. Chem. C*, 2013, **117**, 14778-14786.
28 W. Ma, H. Yin, L. Xu, X. Wu, H. Kuang, L. Wang and C. Xu, *Chem. Commun.*, 2014, **50**, 9737-9740.
29 K. S. Krishna, C. S. S. Sandeep, R. Philip and M. Eswaramoorthy, *ACS Nano*, 2010, **4**, 2681-2688.
30 H. Liu and Q. Yang, *J. Mater. Chem.*, 2011, **21**, 11961-11967.
31 S. Tang, S. Vongehr, Y. Wang, J. Cui, X. Wang and X. Meng, *Mater. Chem. A*, 2014, **2**, 3648-3660.
32 B. C. Galarreta, I. Rupar, A. Young and F. Lagugné-Labarthet, *J. Phys. Chem. C*, 2011, **115**, 15318-15323.
33 D. Correia-Ledo, K. F. Gibson, A. Dhawan, M. Couture, T. Vo-Dinh, D. Graham and J.-F. Masson, *J. Phys. Chem. C*, 2012, **116**, 6884-6892.
34 S. F. Parker, *Chem. Phys.*, 2013, **424**, 75-79.
35 C. Blum, T. Schmid, L. Opilik, S. Weidmann, S. R. Fagerer and R. Zenobi, *J. Raman Spectrosc.*, 2012, **43**, 1895-1904.
36 L. Tong, T. Zhu and Z. Liu, *Chem. Soc. Rev.*, 2011, **40**, 1296-1304.